Enhanced lasing from organic gain medium by Au nanocube@SiO₂ core-shell nanoparticles with optimal size

SHUYA NING,^{1,5} NAMING ZHANG,^{2,6} HUA DONG,³ XUN HOU,³ FANGHUI ZHANG,¹ AND ZHAOXIN WU^{3,4}

⁶namingzhang@xjtu.edu.cn

Abstract: We report a dramatic enhancement of random lasing assisted by Au nanocube-silica core-shell nanoparticles (Au NC@SiO₂ NPs) with optimal size. To determine which size of Au NC@SiO₂ NPs would have the optimal plasmon effect, we first investigated the lasing properties based on different sizes of bare Au nanocubes (Au NCs) with different localized surface plasmon resonance (LSPR) spectra; the edge lengths of the Au NCs ranged from 20 nm to 120 nm. The 80 nm Au NCs, whose LSPR spectrum had the largest overlap with the emission spectrum of the gain medium, exhibited the strongest scattering and electric field intensity to better enhance the lasing. Compared to the gain media with bare Au nanocubes or Au nanosphere@SiO₂ nanoparticles, the gain medium with optimally sized Au nanocube @SiO₂ NPs had the lowest lasing threshold, only 21.7% of that of the neat gain medium. This was attributed to the stronger scattering and electric field enhancement localized at the spiky tips of the Au NCs, and the fact that the SiO₂ shell reduced the absorption loss of the dyes in close proximity to the Au NCs. Using the proper size of Au NC@SiO₂ NPs provides an ideal way to achieve low-threshold plasmon random lasing by tuning the LSPR of metallic nanostructures.

© 2018 Optical Society of America under the terms of the OSA Open Access Publishing Agreement

OCIS codes: (140.3460) Lasers; (250.5403) Plasmonics; (290.4210) Multiple scattering.

References and links

- M. A. Noginov, G. Zhu, A. M. Belgrave, R. Bakker, V. M. Shalaev, E. E. Narimanov, S. Stout, E. Herz, T. Suteewong, and U. Wiesner, "Demonstration of a spaser-based nanolaser," Nature 460(7259), 1110–1112 (2009).
- R. F. Oulton, V. J. Sorger, T. Zentgraf, R. M. Ma, C. Gladden, L. Dai, G. Bartal, and X. Zhang, "Plasmon lasers at deep subwavelength scale," Nature 461(7264), 629–632 (2009).
- H. A. Atwater and A. Polman, "Plasmonics for improved photovoltaic devices," Nat. Mater. 9(3), 205–213 (2010).
- H. Dong, Z. X. Wu, J. Xi, X. Xu, L. Zuo, T. Lei, X. Zhao, and X. Hou, "Pseudohalide-induced recrystallization engineering for CH₃NH₃PbI₃ film and its application in highly efficient inverted planar heterojunction perovskite solar cells," Adv. Funct. Mater. 28(2), 1704836 (2018).
- M. I. Stockman, "Spasers explained," Nat. Photonics 2(6), 327–329 (2008).
- O. Popov, A. Zilbershtein, and D. Davidov, "Enhanced amplified emission induced by surface plasmons on gold nanoparticles in polymer film random lasers," Adv. Technol. 18(9), 751–755 (2007).
- S. Y. Ning, Z. X. Wu, H. Dong, and F. H. Zhang, "Enhancement of lasing in organic gain media assisted by the metallic nanoparticles-metallic film plasmonic hybrid structure," J. Mater. Chem. C 4(24), 5717–5724 (2016).
- G. D. Dice, S. Mujumdar, and A. Y. Elezzab, "Plasmonically enhanced diffusive and subdiffusive metal nanoparticles-dye random laser," Appl. Phys. Lett. 86(13), 131105 (2005).
- X. Meng, K. Fujita, Y. Zong, S. Murai, and K. Tanaka, "Random lasers with coherent feedback from highly transparent polymer films embedded with silver nanoparticles," Appl. Phys. Lett. 92(20), 201112 (2008).

¹College of Electrical and Information Engineering, Shanxi University of Science and Technology, Xi'an 710021, China

²School of Electrical Engineering, Xi'an Jiaotong University, Xi'an 710049, China

³Key Laboratory of Photonics Technology for Information, School of Electronic and Information Engineering, Xi'an Jiaotong University, Xi'an 710049, China

⁴Collaborative Innovation Center of Extreme Optics, Shanxi University, Taiyuan 030006, China

³ningshuya@sust.edu.cn

- 10. X. Meng, K. Fujita, S. Murai, and K. Tanaka, "Coherent random lasers in weakly scattering polymer films containing silver nanoparticles," Phys. Rev. A 79(5), 053817 (2009).
- T. Zhai, X. Zhang, Z. Pang, X. Su, H. Liu, S. Feng, and L. Wang, "Random laser based on waveguided plasmonic gain channels," Nano Lett. 11(10), 4295-4298 (2011).
- E. Heydari, R. Flehr, and J. Stumpe, "Influence of spacer layer on enhancement of nanoplasmon-assisted random lasing," Appl. Phys. Lett. 102(13), 133110 (2013).
- W. Ismail, E. Goldys, and J. Dawes, "Plasmonic enhancement of Rhodamine dye random lasers," Laser Phys. 25(8), 085001 (2015).
- 14. O. Popov, A. Zilbershtein, and D. Davidov, "Random lasing from dye-gold nanoparticles in polymer films: Enhanced gain at the surface-plasmon-resonance wavelength," Appl. Phys. Lett. 89(19), 191116 (2006).
- T. Zhai, J. Chen, L. Chen, J. Wang, L. Wang, D. Liu, S. Li, H. Liu, and X. Zhang, "A plasmonic random laser tunable through stretching silver nanowires embedded in a flexible substrate," Nanoscale 7(6), 2235–2240
- 16. X. Wu, T. Ming, X. Wang, P. Wang, J. Wang, and J. Chen, "High-photoluminescence-yield gold nanocubes: for cell imaging and photothermal therapy," ACS Nano 4(1), 113–120 (2010).

 Y. Cui, C. Niu, N. Na, and J. Ouyang, "Core–shell gold nanocubes for point mutation detection based on
- plasmon-enhanced fluorescence," J. Mater. Chem. B Mater. Biol. Med. 5(27), 5329-5335 (2017).
- 18. R. Frank, A. Lubatsch, and J. Kroha, "Theory of strong localization effects of light in disordered loss or gain media," Phys. Rev. B 73(24), 245107 (2006).
- 19. X. Meng, K. Fujita, S. Murai, T. Matoba, and K. Tanaka, "Plasmonically controlled lasing resonance with metallic-dielectric core-shell nanoparticles," Nano Lett. 11(3), 1374-1378 (2011).
- 20. X. Meng, K. Fujita, Y. Moriguchi, Y. Zong, and K. Tanaka, "Metal-dielectric core-shell nanoparticles: advanced plasmonic architectures towards multiple control of random lasers," Adv. Opt. Mater. 1(8), 573–580 (2013). 21. P. Johnson and R. Christy, "Optical constants of the noble metals," Phys. Rev. B 6(12), 4370–4379 (1972).
- 22. E. M. Perassi, C. Hrelescu, A. Wisnet, M. Döblinger, C. Scheu, F. Jäckel, E. A. Coronado, and J. Feldmann, "Quantitative understanding of the optical properties of a single, complex-shaped gold nanoparticle from experiment and theory," ACS Nano 8(5), 4395-4402 (2014).
- 23. C. Hrelescu, T. K. Sau, A. L. Rogach, F. Jäckel, G. Laurent, L. Douillard, and F. Charra, "Selective excitation of individual plasmonic hotspots at the tips of single gold nanostars," Nano Lett. 11(2), 402-407 (2011).
- 24. C. Hrelescu, T. K. Sau, A. L. Rogach, F. Jäckel, and J. Feldmann, "Single gold nanostars enhance Raman scattering," Appl. Phys. Lett. 94(15), 153113 (2009).
- 25. X. Shi, Y. Wang, Z. Wang, S. Wei, Y. Sun, D. Liu, and J. Shi, "Random lasing with a high quality factor over the whole visible range based on cascade energy transfer," Adv. Optical Mater. 2(1), 88-93 (2014).
- J. Ziegler, M. Djiango, C. Vidal, C. Hrelescu, and T. A. Klar, "Gold nanostars for random lasing enhancement," Opt. Express 23(12), 15152-15159 (2015).

1. Introduction

Recently, random lasers based on plasmonic metal nanoparticles (NPs) have attracted significant attention because of their interesting physical mechanism and potential values in applications [1–5]. It had been demonstrated that metal NPs are always beneficial to lasing efficiency via the two mechanisms of the enhanced localized electric field and scattering effects [6,7]. Therefore, many researchers had reported utilizing metal NPs to obtain higher efficiency random lasing. For example, Dice et al. demonstrated plasmonic enhancement of lasing properties in a random laser based on a suspension containing Rhodamine 6G (R6G) and 55 nm silver NPs [8]. Meng et al. reported enhanced lasing in the gain medium by introducing silver NPs of a certain size [9,10]. Zhai et al. showed a threshold reduction for a waveguide-plasmonic scheme constructed by coating the gain medium onto gold NPs [11]. Heydari et al. reported enhanced lasing in a gold NP-based random laser by tuning the coupling between the gain material and the localized surface plasmon resonance (LSPR) of Au NPs [12]. In addition, Ismail et al. reported improved characteristics in a random laser with 60 nm gold NPs [13]. Surface plasmon enhancement of the lasing properties is expected to be optimal when the LSPR of metal NPs overlaps well with the emission of gain medium [12,14,15]. However, in those prior works, we found that the plasmonic random lasers were mostly based on bare spherical metal NPs of a given size. And these given spherical metal NPs offered the LSPR spectrum, which may be not optimally matched with the emission spectrum of the gain medium; this would cause the corresponding nanospheres to exhibit a weak localized electric field and insufficient scattering effects. It means that two problems must be solved: 1) It is especially desired to develop the other shape of metal NPs with stronger localized electric field and scattering effects. 2) It should be determined the optimal

size of metal NPs with proper LSPR spectrum to better match the emission spectrum of the gain medium, so as to achieve the stronger plasmon coupling effect to further optimize random lasing performance.

Here, we prepared the unique Au nanocube-silica core-shell nanoparticles (Au NC@SiO₂ NPs) with an optimal size and introduced it into the gain medium to enhance the lasing properties. Because of the strong dependence of lasing threshold on the size of nanoparticles, it is necessary to confirm the optimal size of the Au NC@SiO₂ NPs. We first studied the effects of different sizes of bare Au nanocubes (Au NCs) with different LSPR spectra on lasing properties. The edge lengths of the Au NCs ranged from 20 nm to 120 nm, and the 80 nm Au NCs showed the optimal plasmon effect to enhance the lasing. This occurred because the corresponding LSPR spectrum of 80 nm Au NCs had the largest overlap with the emission spectrum of the gain medium, so that the 80 nm Au NCs exhibited the strongest scattering and electric field than the other sizes of Au NCs. This indicated the optimal size of the Au NC@SiO₂ NPs. Compared to the bare Au nanocubes or Au nanosphere-silica coreshell nanoparticles (Au nanosphere@SiO₂ NPs), the optimally sized Au nanocube@SiO₂ NPs could better enhance the lasing properties and lower the lasing threshold. This was attributed to the stronger scattering and electric field intensity due to the unique "plasmonic hot spot" characteristic of Au NCs, and the fact that the SiO₂ shell could reduce the absorption loss of the dyes in close proximity to the bare Au NCs. Our strategy provided here suggests that Au NC@SiO₂ NPs can serve as promising candidate toward the development of highly efficient plasmon-based random laser.

2. Sample preparation and experimental setups

In order to determine the optimal size for the Au NC@SiO₂ NPs, we first investigated the effects on the lasing characteristics caused by different sizes of bare Au NCs. The Au NCs were prepared by adopting a seed-mediated growth method in aqueous cetyltrimethylammonium bromide (CTAB) solution [16,17]. Figure 1 shows the transmission electron microscopy (TEM) images of Au NCs with the edge lengths of 20, 60, 80, 100, and 120 nm.

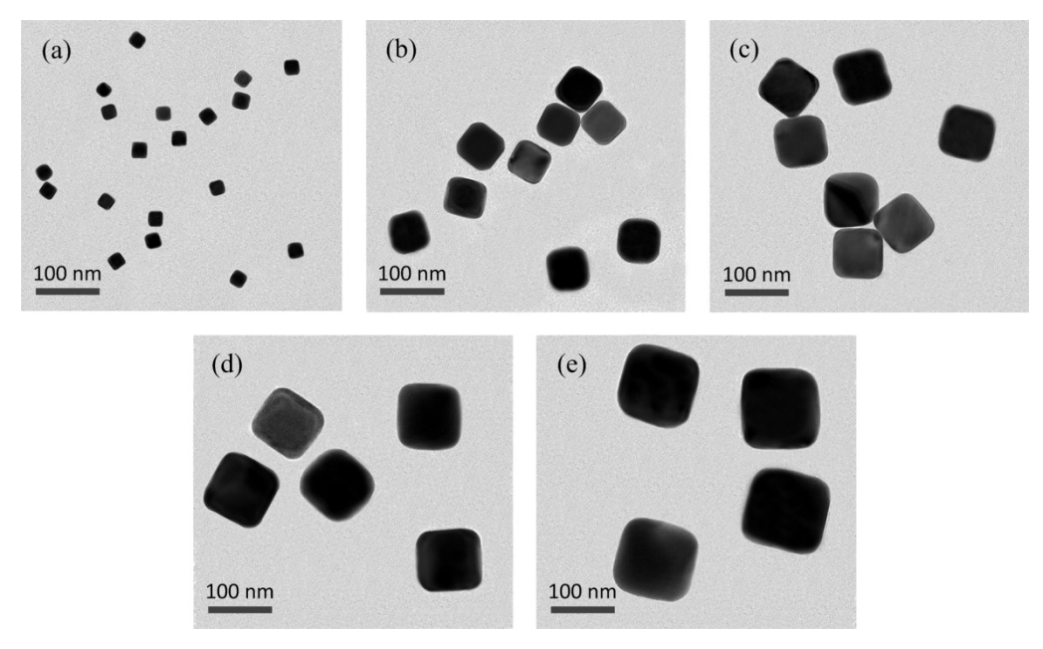


Fig. 1. The TEM images of Au NCs with different sizes. The average edge lengths of the Au NCs are (a) 20 nm, (b) 60 nm, (c) 80 nm, (d) 100 nm, and (e) 120 nm.

The emission material was based on a polymer film prepared by fully dissolving polystyrene (PS) polymer (20 mg/mL) and R6G dyes (3 mM) in chloroform. Then the different sizes of Au NCs were doped into the dye solutions with a constant mass concentration of 5.56×10^{-4} g/cm³ (corresponding to the mass filling fraction of $3.7 \times 10^{-4\%}$) [18]. The different blend solutions (1 mL) were spin-coated onto glass substrates at a speed of 2000 rpm for 30 seconds. And the spin-coated films were annealed at 110 °C for 10 min to remove the solvent. The size of the glass substrate was about 2.5 cm \times 3.5 cm. For comparison, we also prepared a reference sample containing no NPs. The thicknesses of the gain medium films were about 400 nm. Figure 2 shows the structure of a device with Au NCs.

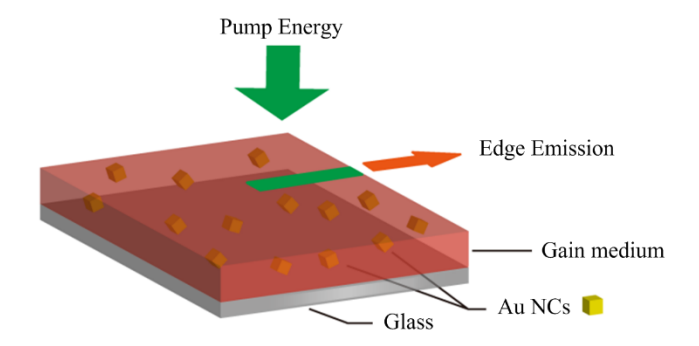


Fig. 2. The structure of a device whose gain medium had been doped with Au NCs.

In the experiments, the absorption and photoluminescence spectra were obtained with a UV-Vis spectrophotometer (HITACHI U-3010, Japan) and a fluorescence spectrometer (Fluoromax-4). The polymer thicknesses were measured with an ellipsometer (SE MF-1000, Korea). The devices were photopumped at normal incidence with an Nd:YAG laser (532 nm, 10 Hz repetition rate, and 5.5 ns pulse duration). An adjustable slit and a cylindrical lens were used to shape the beam into a 7 mm × 1 mm stripe. The edge emission spectra were measured with a fiber optic spectrometer (Ocean Optics SpectraSuite, USB2000).

3. Results and discussion

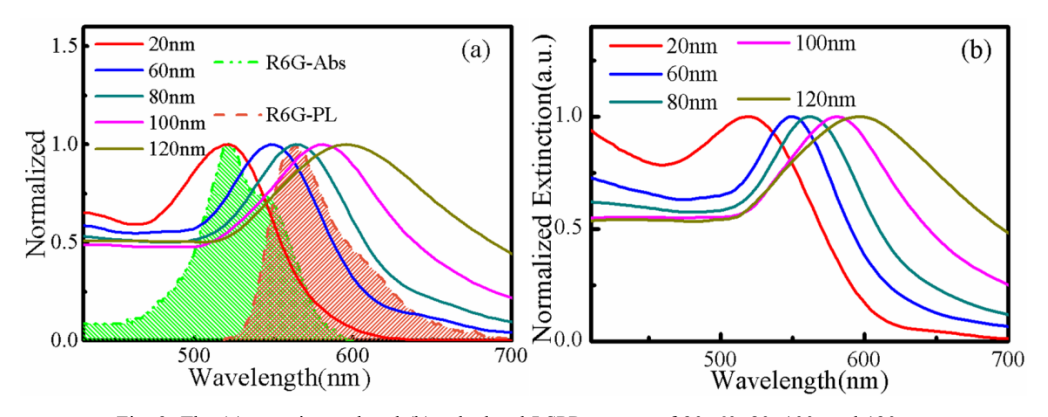


Fig. 3. The (a) experimental and (b) calculated LSPR spectra of 20, 60, 80, 100, and 120 nm Au NCs; the absorption and emission spectra of R6G are included in (a).

We know that the LSPR spectrum of metallic NPs strongly depends on the material, its size and shape, and the surrounding environment; therefore, the variation of one or more of these parameters allows spectral tuning of the plasmon resonance to couple with the gain medium. Here, in order to develop appropriately sized Au NCs with proper LSPR that could then be used for preparing Au NC@SiO₂ NPs, we first fabricated the different sizes of Au NCs.

Figure 3(a) presents the LSPR spectra of different sizes of Au NCs in PS polymer, together with the absorption and emission spectra of R6G. Clearly, the LSPR peaks show redshift from 518 nm to 595 nm as the edge lengths of the Au NCs vary from 20 nm to 120 nm. To further determine the LSPR spectra of Au NCs, we calculated the normalized extinctions of different sizes of single Au NC in PS polymer without dye background using Mie theory with the finite difference time domain (FDTD) method, as shown in Fig. 3(b). The good agreement between experiment and calculation suggests the uniform size and shape distribution of Au NCs. Different sizes of Au NCs have different LSPR spectra, which have different overlaps with the absorption and emission spectra of the gain medium, suggesting the different coupling between Au NCs and gain material.

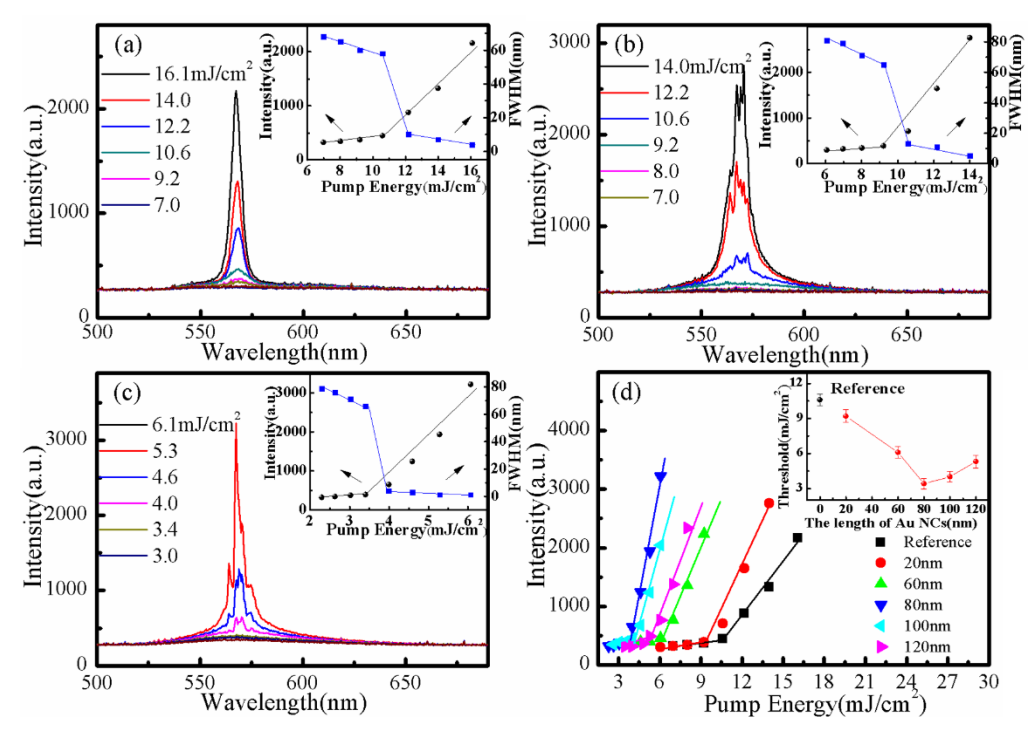


Fig. 4. Emission spectra of the devices with (a) no metallic NPs, (b) 20 nm Au NCs, and (c) 80 nm Au NCs; the corresponding lasing intensities and FWHMs of the emission spectra are shown in the insets of (a) to (c). (d) Dependences of the emission intensity on the pump energy for different devices, the inset shows the lasing thresholds of different devices.

To determine the optimal size of Au NC@SiO₂ NPs, we first studied the effects of different sizes of bare Au NCs on the lasing characteristics. And we prepared the devices with 20, 60, 80, 100, and 120 nm Au NCs, while maintaining the constant mass concentration of 5.56 × 10⁻⁴ g/cm³. For comparison, the lasing properties of the reference device without any metal NPs were investigated. Figure 4(a) shows the emission spectra of the reference device as a function of the pump energy. At first, the emission spectrum is broad, and the emission intensity increases slowly with the increase in pump intensity; as the pump energy exceeds the lasing threshold, the emission spectrum becomes narrow with a sharp increase of the emission intensity. The inset of Fig. 4(a) shows the rapid decrease in full width at half maximum (FWHM) of the emission spectrum above the threshold, which is 10.6 mJ/cm². Figure 4(b) and (c) show the emission spectra of the devices based on 20 nm and 80 nm Au NCs excited at different pump energies; they all show the coherent random lasing phenomenon as indicated by the emergence of sharp spikes in the emission spectra after the introduction of the Au NCs. The threshold behaviors are shown in the insets of Fig. 4(b) and

(c), respectively. Figure 4(d) illustrates the emission intensity as a function of pump energy for devices with different sizes of Au NCs. The corresponding lasing thresholds are presented in the inset of Fig. 4(d), which shows that the lasing threshold reduces with the increased Au NC size, but with further increased Au NC size, the lasing threshold increases. We found that the lowest lasing threshold is 3.4 mJ/cm² for the gain medium with 80 nm Au NCs, whose LSPR spectrum overlaps completely with the emission spectrum of the gain medium, as shown in Fig. 3(a).

According to the studies above, we can know that the 80 nm bare Au NCs could better enhance the random lasing performance. However, when the dye molecules are in close proximity to the metallic surface, there is extremely high absorption loss that is detrimental to lasing [19,20]. Therefore, after the optimal size of bare Au NC was determined, we prepared the Au NC@SiO₂ NPs comprising the 80 nm Au nanocube core coated with 7 nm SiO₂ shell as shown in the inset of Fig. 5(a); the silica coating on the surface of the Au NCs was prepared by a modified Stöber method [17]. To further determine the advantages of Au NC@SiO₂ NPs on lasing, we doped the Au NC@SiO₂ NPs into the gain medium with the same number density as that of the 80 nm Au NCs in the gain medium above, the mass filling fraction of the Au NC@SiO₂ NPs was 3.93 × 10^{-4%}. For comparison purposes, we developed a related experiment associated with Au nanosphere@SiO₂ NPs (80 nm in diameter @7 nm) [shown in the inset of Fig. 5(c)] instead of Au nanocube@SiO₂ NPs. Figure 5(a) and (c) depict the emission spectra of the devices based on Au nanocube @SiO2 NPs and Au nanosphere@SiO₂ NPs, respectively. The corresponding emission intensities and FWHMs for these two samples are shown in Fig. 5(b) and (d); they exhibit lasing thresholds of 2.3 mJ/cm² and 5.3 mJ/cm², respectively. According to Figs. 4 and 5, compared to the devices based on bare Au nanocubes or Au nanosphere@SiO2 NPs, the device with Au nanocube@SiO2 NPs has the lowest lasing threshold, which is only about 21.7% of that of the reference device. This demonstrates that the Au nanocube@SiO₂ NPs can enhance stimulated emission to a much higher degree than the bare Au nanocubes or Au nanosphere@SiO₂ NPs.

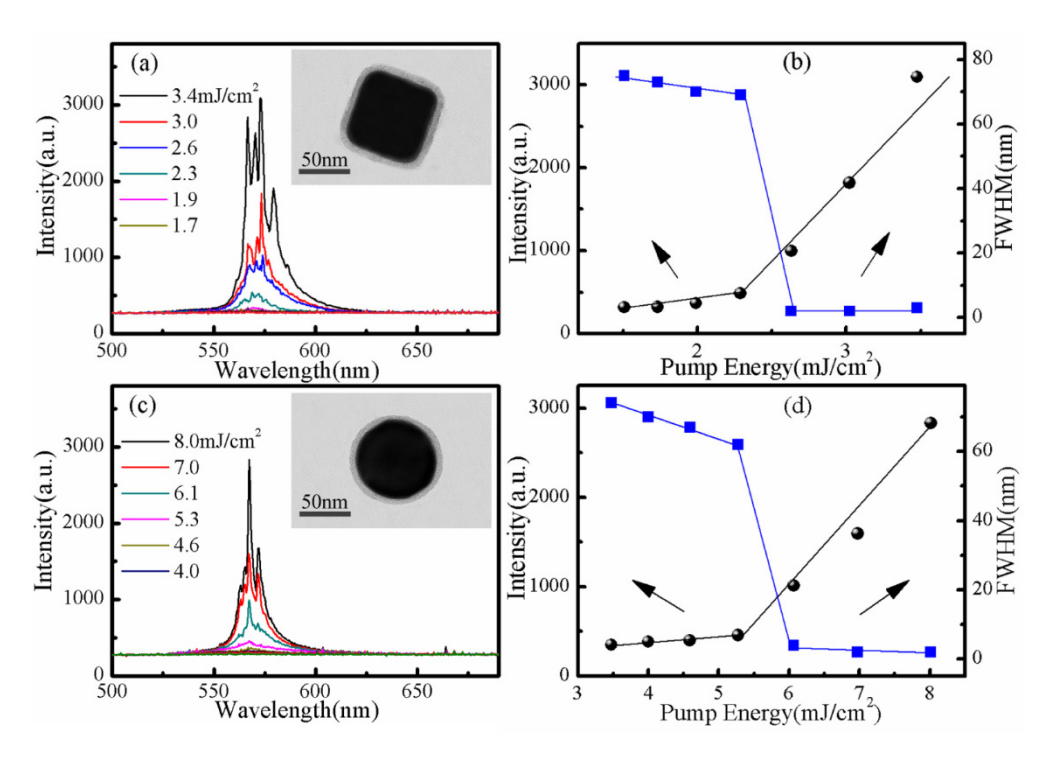


Fig. 5. Emission spectra of the devices with (a) Au nanocube@SiO₂ NPs, (c) Au nanosphere@SiO₂ NPs; (b) and (d) the lasing intensities and FWHMs of the emission spectra corresponding to (a) and (c). The insets in (a) and (c) show the TEM images of Au nanocube@SiO₂ NP and Au nanosphere@SiO₂ NP.

We know that the metallic nanoparticles can enhance the lasing by two separate mechanisms: the enhanced localized electric field and scattering [6,7]. In order to explore the essential cause of the experiment results above and further identify it, we calculated the enhanced localized electric field and scattering of an Au nanosphere and different sizes of Au nanocubes, respectively.

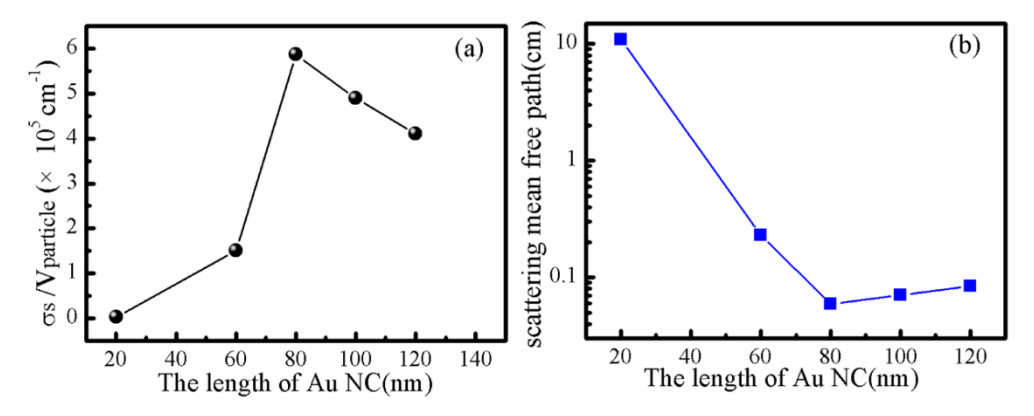


Fig. 6. (a) The normalized scattering cross section of different sizes of Au NCs at $\lambda = 570$ nm, (b) the scattering mean free paths at $\lambda = 570$ nm, as a function of the size of Au NC.

For one mechanism of scattering, due to the equal mass concentration of different sizes of Au NCs in the gain medium, $\sigma_s/V_{\text{particle}}$ was calculated as a normalized scattering cross section to evaluate the scattering strength of different sizes of Au NCs; σ_s is the scattering cross section, and V_{particle} is the particle volume. Figure 6(a) shows the $\sigma_s/V_{\text{particle}}$ of different sizes of

Au NCs at the emission wavelength of 570 nm; it shows that with the increase of the Au NC size, $\sigma_s/V_{\text{particle}}$ increases at first, and then decreases. There is a maximum of $\sigma_s/V_{\text{particle}}$ for the Au NC with an edge length of 80 nm. Moreover, Fig. 6(b) shows the scattering mean free path, l_s , at a wavelength of 570 nm, as a function of the size of Au NCs. The scattering mean free path can be estimated via the Mie theory $l_s = 1/\rho\sigma_s$, where ρ is number density of nanostructure [14,19]. With the increase of the Au NC size, the l_s exhibits the same trend with the lasing threshold. There is the minimum of l_s for the sample with 80 nm Au NCs. The scattering strength is inversely proportional to the l_s , then the 80 nm Au NCs had the strongest scattering strength. In addition, for the devices with Au nanocube@SiO2 NPs(80 nm in edge length @7 nm) or Au nanosphere@SiO₂ NP (80 nm in diameter @7 nm), there were different mass filling fractions of NPs, which were $3.93 \times 10^{-4\%}$ and $2.06 \times 10^{-4\%}$, respectively. According to the scattering cross section of the Au nanocube@SiO₂ NPs $(4.37 \times 10^{-10} \text{ cm}^2)$ and that of the Au nanosphere@SiO₂ NPs $(4.11 \times 10^{-11} \text{ cm}^2)$ at the wavelength of 570 nm, the scattering mean free path l_s for the random laser with Au nanocube@SiO₂ NPs is 0.04 cm, and that with Au nanosphere@SiO₂ NPs is 0.43 cm. Therefore, the Au nanocube@SiO₂ NPs have a stronger scattering than Au nanosphere@SiO₂ NPs.

It is generally known that the localized electric field enhancement near the surface of metal NPs, which results in the enhanced gain region at the particle's surface, could lead to larger amplification of emission light and excite a larger number of such dye molecules at the same time to higher energy levels. And the quantum yields of dye molecules are increased by changing the radiative and nonradiative decay rates [8].

To explore another mechanism of the enhanced localized electric field, we simulated the electric field distributions of the different sizes of Au NCs using the FDTD method. In the simulation, the simulation region was much larger than the sizes of Au NCs and considered as an infinite space. The excitation beam was a plane wave polarized along the x-axis with the wavelength of 570 nm. The permittivity of Au was taken from the experimental data of Johnson and Christy [21]. In order to obtain the high accuracy simulation, the mesh size was set as 1 nm. Figure 7(a)-(e) show the electric field distributions of the different sizes of Au NCs in PS polymer at the wavelength of 570 nm. For the samples with Au NCs, when the dye molecules were excited, the emission wavelength was 570 nm, and in return, the lasing emission wavelength of 570 nm could excite the electric field effect of different sizes of Au NCs, then the strong electric fields of the Au NCs influence the optical properties of the dye molecules in close vicinity of them [15,19,20]. The different electric fields of different sizes of Au NCs would have different effects on lasing dyes. Figure 7 shows that with increasing Au NC size, the electric field enhancement increases at first, and then decreases. The strongest electric field occurs when the edge length of the Au NC is 80 nm, leading to the maximum gain at the lasing emission wavelength. In addition, compared to the case of an 80 nm Au nanosphere shown in Fig. 7(f), the 80 nm Au nanocube has stronger electric field because of the unique "plasmonic hot spot" characteristic that results from the extremely high field enhancement at the corners of Au NCs. This enhanced local field occurring at hot spots is particularly important to effectively augment interactions with nearby molecules and trigger low-threshold lasing resonance [15,19,22–26]. Hence, for the different sizes of Au NCs, the strongest resonant coupling arises between the dye molecules and metallic nanoparticles whose LSPR spectrum overlaps sufficiently with the emission spectrum of the gain medium. Moreover, the superiority of the Au nanocube@SiO₂ NPs over Au nanosphere@SiO₂ NPs can be explained by stronger multiple scattering and superior field enhancement.

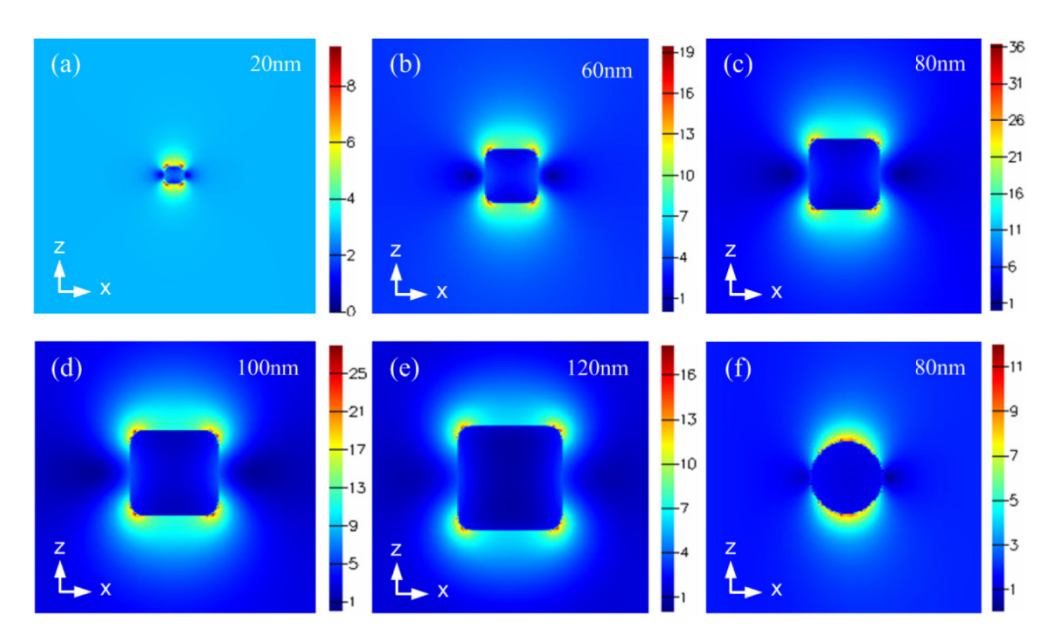


Fig. 7. Electric field distributions of (a) 20 nm, (b) 60 nm, (c) 80 nm, (d) 100 nm, (e) 120 nm Au nanocube; and (f) an 80 nm Au nanosphere at the incident wavelength of 570 nm.

4. Conclusion

In summary, we have demonstrated enhanced random lasing from organic dyes doped with optimally sized Au NC@SiO₂ NPs. In order to find the optimal size for Au NC@SiO₂ NPs with suitable LSPR spectra to match the gain medium, we studied the effects on lasing properties of different sizes of bare Au NCs with different LSPR spectra. The 80 nm Au NCs showed the best plasmon effect to enhance the lasing. This result strongly suggested that surface-plasmon-enhanced lasing properties are expected to be optimal when the LSPR spectrum of metal nanoparticles has sufficient overlap with the lasing emission spectrum, which can lead to stronger localized electric field enhancement and scattering effects of nanoparticles. Compared to the bare Au nanocubes or Au nanosphere@SiO₂ NPs, the optimally sized Au nanocube@SiO₂ NPs more effectively enhanced the lasing properties and lowered the lasing threshold. This was due to the stronger scattering and electric field enhancement localized at the spiky tips of the Au NCs; moreover, the presence of the SiO₂ shell prevented the quenching of the dyes in close proximity to the bare Au NCs, thereby attaining better enhancement. Thus, our work provides an ideal method to reduce the lasing threshold of gain media.

Funding

National Natural Science Foundation of China (61605105); Scientific Research Program Funded by Shaanxi Provincial Education Department (16JK1085); General Financial Grant from the China Postdoctoral Science Foundation (2017M620456); Scientific Research Fund of Shaanxi University of Science and Technology (2016BJ-02).